Revised Version

LPTHE Orsay 98/27
DESY 98-086

hep-ph/9807258 v3 23 Oct 1998

Charmonium Suppression in Lead-Lead Collisions: Is There a Break in the J/ψ Cross-Section?

N. Armesto

II. Institut für Theoretische Physik, Universität Hamburg,

Luruper Chaussee 149, D-22761 Hamburg, Germany

A. Capella and E. G. Ferreiro

Laboratoire de Physique Théorique et Hautes Energies,

Université de Paris-Sud, Bâtiment 211, F-91405 Orsay Cedex, France

Abstract

In the framework of a model based on nuclear absorption plus comover interaction, we compute the E_T distribution of the J/ψ in $PbPb$ collisions at SPS and compare it with available NA50 data. Our analysis suggests that the existence of new physics (deconfinement phase transition) in the region $E_T \lesssim 100$ GeV is unlikely and that signals of new physics should rather be searched in the region $E_T \gtrsim 100$ GeV. The E_T dependence of the J/ψ transverse momentum has been computed. At large E_T it turns out to be much flatter in the comover approach than in a phase transition framework. Estimates of the J/ψ suppression at RHIC and LHC energies are also given.

LPTHE Orsay 98/27

DESY 98-086

hep-ph/9807258

September 1998

1 Introduction

The 1995 data from the NA50 Collaboration [1] show an anomalous J/ψ suppression, i.e. a suppression larger than the one expected in a nuclear absorption model. This model describes the J/ψ suppression both in proton-nucleus interactions and in nucleus-nucleus interactions with a light projectile [1]. Following the original proposal of [2], the anomalous J/ψ suppression has been interpreted as a signal of a deconfining phase transition [3, 4, 5, 6]. However, an explanation by a more conventional mechanism, namely, the interaction of the J/ψ (or the $c\bar{c}$ pair) with comovers, is also possible [7, 8, 9, 10].

A very spectacular feature of the 1996 data by the same Collaboration [11], is the presence of a break in the ratio $R(E_T)$ of J/ψ over Drell-Yan (DY) cross-sections at $E_T \sim$ 55 GeV. It has been argued [12, 6] that this break is a signal of deconfinement – although there is no general consensus on this point [13, 3, 4, 5, 6]. It is, however, fully recognized that a break in the J/ψ cross-section would rule out any conventional model, such as the one based on comover interaction. (Other approaches to J/ψ suppression can be found in [14].)

At present, the evidence for this break is weakened by the presence of fluctuations in the ratio $R(E_T)$ (see Eq. (14) for a precise definition) at large values of E_T [11], which are generally regarded as spurious. Also, it is necessary to assess whether this break, if confirmed, is due to a genuine break in the J/ψ cross-section or rather to fluctuations in the J/ψ and DY ones. Of course, a definitive answer to these questions can only come from data. However, in view of the interest of the subject, it is important to examine the available data in a theoretical framework in order to gain some insight on these questions, while waiting for a complete analysis of the 1996 NA50 data, and above all, for the 1998 results.

The aim of the present work is to perform such an analysis in the framework of a model based on nuclear absorption plus comover interaction. This work is a continuation of the one in Ref. [9]. We use the same formalism and the same values of the parameters which were determined in [9] from the best fit to the ratio $R(E_T)$ in pA, SU and $PbPb$ collisions. The plan of the paper is the following. In Section 2 we describe the model. In Section 3 we compute the E_T distributions of minimum bias, DY and J/ψ, and compare them with available data. In Section 4 we compute the ratio $R(E_T)$ and compare it with the NA50 data. In Section 5 we compute the E_T dependence of the average p_T^2 of the J/ψ

and compare it with recent NA50 data. Section 6 contains our conclusions and prospects at higher energies.

2 The model

Our model is formulated in a conventional framework [7, 8, 9, 10] based on two different mechanisms of J/ψ suppression: nuclear absorption of the pre-resonant $c\bar{c}$ pair with nucleons of the colliding nuclei and absorption by comoving partons or hadrons produced in the collision. For completeness we recall its main ingredients:

Nuclear absorption: In nucleus-nucleus collisions, the survival probability of the J/ψ at impact parameter b and transverse position s is given by [15, 9]

$$S^{abs}(b,s) = \frac{[1-\exp(-A\ T_A(s)\ \sigma_{abs})][1-\exp(-B\ T_B(b-s)\ \sigma_{abs})]}{\sigma_{abs}^2\ AB\ T_A(s)\ T_B(b-s)} \quad . \tag{1}$$

Here $T_{A(B)}(b) = \int_{-\infty}^{+\infty} dz\ \rho_{A(B)}(b,z)$ are the nuclear profile functions normalized to unity. The nuclear densities $\rho_{A(B)}(b,z)$ are determined from a 3-parameter Fermi distribution with parameters given in Ref. [16]. (In Ref. [9] a different parametrization of the nuclear density is used; this introduces differences in $R(E_T)$ of less than 4 % in $PbPb$ collisions.) For the absorptive cross-section we take $\sigma_{abs} = 6.7 \div 7.3$ mb, consistent with a fit to the proton-nucleus data [5]. Note that $S^{abs} = 1$ for $\sigma_{abs} = 0$.

Absorption by comovers. This absorption is due to the interaction of the $c\bar{c}$ pair (or of the J/ψ itself) in the dense medium produced in a nucleus-nucleus collision – which results in the production of a $D\overline{D}$ pair. The J/ψ survival probability is given by [5, 9]

$$S^{co}(b,s) = \exp\left[-\sigma_{co}\ N_y^{co}(b,s)\ \ln\left(\frac{N_y^{co}(b,s)}{N_f}\right)\ \theta(N_y^{co}(b,s) - N_f)\right] \quad . \tag{2}$$

Here $N_y^{co}(b,s)$ is the initial density of comovers per unit transverse area d^2s and per unit rapidity at impact parameter b, and N_f is the corresponding freeze-out density. In order to have a smooth onset of the comovers, it is natural to take for N_f the density of hadrons per unit rapidity in a pp collision, i.e. $N_f = [3/(\pi R_p^2)]\ dN^-/dy|_{y^*=0} = 1.15$ fm^{-2}. This coincides with the value introduced in Ref. [5]. With this choice of N_f, the θ-function in Eq. (2) is numerically irrelevant. The effect of the comovers in pA turns out to be negligibly small. σ_{co} is the comover cross-section properly averaged over the momenta of the colliding particles (the relative velocity of the latter is included in its definition). The logarithmic factor in Eq. (2) is the result of an integration in the proper time τ from the initial time to freeze-out time. (One assumes [17, 18] a decrease of densities with proper time in $1/\tau$.) A large contribution to this integral comes from the few first fm/c after the collision – where the system is in a pre-hadronic stage. (In this respect, see the last paper of Ref. [10].) Actually, Brodsky and Mueller [19] introduced the comover interaction as a coalescence phenomenon at the partonic level. In view of that, there is no precise connection between σ_{co} and the physical $J/\psi - \pi$ or $J/\psi - N$ cross-section, and σ_{co} has to be considered as a free parameter. We take $\sigma_{co} = 0.6$ mb [9].

Cross-sections: The J/ψ production cross-section in nuclear collisions is given by

$$\sigma^{\psi}_{AB}(b) = \frac{\sigma^{\psi}_{pp}}{\sigma_{pp}} \int d^2s \ m(b,s) \ S^{abs}(b,s) \ S^{co}(b,s) \quad , \tag{3}$$

where

$$m(b,s) = AB \ \sigma_{pp} \ T_A(s) \ T_B(b-s) \quad . \tag{4}$$

We take $\sigma_{pp} = 30$ mb. With the definition (3), the Drell-Yan cross-section (obtained from (3) with $\sigma_{abs} = \sigma_{co} = 0$) is proportional to AB.

The cross-section for minimum bias (MB) events is given by

$$\sigma_{AB}(b) = 1 - \exp[-\sigma_{pp} \ AB \ T_{AB}(b)] \quad , \tag{5}$$

with $T_{AB}(b) = \int d^2s \ T_A(s) T_B(b-s)$.

In order to compute these cross-sections we need to know the comover density $N^{co}_y(b,s)$ in the NA50 dimuon spectrometer. Moreover, comparison with experiment requires to compute the above cross-section at a given transverse energy E_T – measured in the NA50 calorimeter. This requires the knowledge of the $E_T - b$ correlation function $P(E_T, b)$. In the following we proceed to calculate these two quantities.

Density of comovers: It is commonly assumed in the literature that the density of comovers is proportional to that of participating (or wounded) nucleons [5, 20]. This is the so-called Wounded Nucleon Model (WNM; for a review see [21]). In asymmetric systems and, in particular, in pA collisions, this model provides a reasonable description of the data but only for the average multiplicity – or at negative rapidities, close to the maximum of the rapidity distribution. For symmetric AA collisions, the model seems to be valid in a broader rapidity range. (This can be understood from the arguments in Ref. [22]; see p. 26.) However, for central $PbPb$ collisions (and also for other central nucleus-nucleus collisions at SPS) there is experimental evidence of a violation of this scaling law at mid-rapidities [23, 24]. Moreover, models such as the Dual Parton Model (DPM) [22], in which unitarity is fully implemented, contain an extra term proportional to the average number of collisions. This term is small at present energies but its relative size increases with energy. Moreover, it contributes mostly at mid-rapidities. The origin of this term is the following. In DPM one has both baryonic strings of type diquark-quark and bosonic ones of type q-$\overline{q}$. The latter contribute mainly at mid-rapidities. Since the number of diquarks available is equal to the number of participating nucleons, the number of baryonic strings is equal to the number of participants. On the other hand, the total number of strings is proportional to the number of collisions. Therefore, the number of q-$\overline{q}$ strings increases, with increasing centrality, much faster than the number of participants. The WNM is obtained from DPM by neglecting the contribution of the q-$\overline{q}$ strings.

In the following calculations we will use the density of comovers given by DPM. We will also discuss how the J/ψ suppression is modified when using a density of comovers proportional to the number of participants.

In DPM, $N_y^{co}(b,s)$ is given by [9, 22]

$$\begin{aligned} N_y^{co}(b,s) &= [N_1\ m_A(b,s) + N_2\ m_B(b,b-s) + N_3\ m(b,s)]\,\theta(m_B(b,b-s) - m_A(b,s)) \\ &+ \ [N_1'\ m_A(b,s) + N_2'\ m_B(b,b-s) + N_3'\ m(b,s)]\theta\left(m_A(b,s) - m_B(b,b-s)\right) \quad . \end{aligned} \tag{6}$$

Here m is given by Eq. (4) and m_A, m_B are the well known geometric factors [25, 18]

$$m_{A(B)}(b,s) = A(B)\ T_{A(B)}(s) \left[1 - \exp\left(-\sigma_{pp}\ B(A)\ T_{B(A)}(b-s)\right)\right] \quad . \tag{7}$$

The coefficients N_i and N_i' are obtained in DPM by convoluting momentum distribution functions and fragmentation functions [22]. Their values (per unit rapidity) for the rapidity window and energies of the NA38 and NA50 experiments are given in Table 1 of Ref. [9]. The rapidity density of hadrons is given by

$$\frac{dN^{co}}{dy} = \frac{1}{\sigma_{AB}} \int d^2b \int d^2s\ N_y^{co}(b,s) \quad , \tag{8}$$

with $\sigma_{AB} = \int d^2b\ \sigma_{AB}(b)$. Note that at fixed b in the range of interest, $\sigma_{AB}(b) \simeq 1$.

The obtained densities of negative hadrons at $y^* = 0$ for pp, SS, SAu and $PbPb$ are compared in Table 2 of Ref. [9] with available data, using in each case the centrality criteria (in percentage of total events) given by the experimentalists. In Fig. 1 we compare the predictions of both the DPM and the WNM with the NA49 data [23] for the rapidity distribution of negative particles in central $PbPb$ collisions at 158 AGeV/c.

$E_T - b$ correlation: The experimental results are given as a function of E_T. This is the total transverse energy of neutrals measured by the NA50 calorimeter in the rapidity window $-1.8 < y^* < -0.6$. The correspondence between average values of b and E_T is given by the proportionality between E_T and multiplicity:

$$E_T(b) = q \ N_y^{co}(b) \quad , \tag{9}$$

where $N_y^{co}(b) = \int_{-1.8}^{-0.6} dy \int d^2s \ N_y^{co}(b,s)$, with $N_y^{co}(b,s)$ given by Eq. (6). The parameter q is closely connected to the average transverse energy per particle. However, it contains extra factors due to the fact that N_y^{co} corresponds to the multiplicity of negatives whereas E_T is the transverse energy of neutrals. Moreover, a calibration factor of the NA50 calorimeter (which has an estimated systematic error of about 40 %) is also included in q.

A precise determination of q comes from the measured correlation between E_T and E_{ZDC} – the energy measured at the zero-degree calorimeter. The latter is defined as

$$E_{ZDC}(b) = [A - m_A(b)] \ E_{in} \quad , \tag{10}$$

where $m_A(b) = \int d^2s \ m_A(b,s)$, i.e. the average number of participants of A at fixed impact parameter, and AE_{in} is the beam energy ($E_{in} = 158$ GeV/c). A fit to the experimental $E_T - E_{ZDC}$ correlation using Eqs. (9) and (10) allows a precise determination of q. From the NA50 data [11] we obtain $q = 0.78$ GeV. It follows from (9) and (10) that with the WNM ansatz [5]: $E_T(b) = 0.4 \ [m_A(b) + m_B(b)]$ GeV, the $E_T - E_{ZDC}$ correlation is a straight line. Experimentally, it is indeed found to be close to a straight line but shows a clear concavity. In DPM this correlation has a concavity due to the contribution of the q-$\overline{q}$ strings. However, in the acceptance region of the NA50 E_T calorimeter, the contribution of the q-$\overline{q}$ strings is rather small (see Fig. 1) and the concavity is also small. Actually, DPM describes well the data in the upper half of the E_T region but falls too fast at low E_T – while the WNM describes the data better in the low E_T region (see Fig. 2). One could think that the difference between the two correlation functions is too small to have any significant effect on the shape of the E_T distributions. It turns out that this is not the case and, therefore, a more accurate description of the $E_T - E_{ZDC}$ correlation is needed.

The failure of the DPM at low E_T can be attributed to the effect of the intra-nuclear cascade, which is not included in (6). This well known phenomenon consists in the production of extra particles in the fragmentation regions of the two colliding nuclei due to the rescattering of slow secondaries (in the rest frames of the two nuclei) with spectator nucleons. Obviously this effect has to vanish for central collisions when no spectator nucleons are left. It is also absent at mid-rapidities. However, the rapidity region of the E_T calorimeter $-1.8 < y^* < 0.6$ is affected by the intra-nuclear cascade (which is known to have an extension of about 1.5 rapidity units). In order to incorporate the intra-nuclear cascade in a phenomenological way, we replace Eq. (9) by

$$E_T(b) = q\ N_y^{co}(b) + k\ E_{ZDC}(b) \quad . \tag{9'}$$

With the values of the parameters we use, $q = 0.78$ GeV and $k = 1/4000$, the relative contribution of the second term in (9′) is comparatively small (about 30 % for a very peripheral collision with $E_{ZDC} = 30000$ GeV and less than 2 % for $E_{ZDC} \lesssim 10000$ GeV). The only drawback of this extra term is that it does not vanish at $E_{ZDC} = E_{ZDC}^{MAX} = AE_{in}$. However, this can be easily cured by replacing Eq. (9′) by

$$E_T(b) = q\ N_y^{co}(b) + 0.95 \left(\frac{E_{ZDC}(b)}{4000}\right)^{1.2} \left(\frac{E_{ZDC}^{MAX} - E_{ZDC}(b)}{E_{ZDC}^{MAX}}\right)^{0.2} \quad . \tag{9''}$$

The corresponding $E_T - E_{ZDC}$ correlation, shown in Fig. 2 (full line), is practically identical to the one obtained from (9′) for $E_T < 30000$ GeV and gives an excellent description of the experimental data [11]. Moreover, both correlations lead to the same E_T distributions for J/ψ and DY in the region $E_T \gtrsim 15$ GeV, where data are available. Eq. (9″) will be used in all DPM calculations.

In order to obtain the $E_T - b$ correlation, and not only the relation between the average values of these two quantities, we have to determine the E_T distributions at a given b. A good description of the experimental E_T distributions is obtained [20, 5, 26] using a Gaussian distribution at fixed impact parameter, with squared dispersion $D^2(b) \equiv$

$\langle [N_y^{co}(b)]^2 \rangle - \langle N_y^{co}(b) \rangle^2 = a \langle N_y^{co}(b) \rangle$, i.e.

$$P(E_T, b) = \frac{1}{\sqrt{2\pi q^2 a \overline{N}_y(b)}} \exp\left[- \frac{[E_T - q\overline{N}_y(b)]^2}{2q^2 a \overline{N}_y(b)} \right] \quad , \tag{11}$$

where $\overline{N}_y(b) = E_T(b)/q$, with $E_T(b)$ given by Eq. ($9''$), and a is a free parameter (see Section 3).

3 $\mathbf{E_T}$ distributions

The E_T distributions of J/ψ, DY and Minimum Bias (MB) are obtained by folding the corresponding cross-sections at fixed b (Eqs. (3) and (5)) with the $E_T - b$ correlation function:

$$\frac{d\sigma^\psi}{dE_T} = \int d^2b \ \sigma_{AB}^\psi(b) \ P(E_T, b) \quad , \tag{12}$$

$$\frac{d\sigma^{MB}}{dE_T} = \int d^2b \ \sigma_{AB}(b) \ P(E_T, b) \quad . \tag{13}$$

The corresponding expression for DY is obtained from (12) with $\sigma_{abs} = \sigma_{co} = 0$.

The most precise determination of the parameter a is obtained from a fit of (the tail of) the MB E_T distribution. Using the 1995 data of Ref. [26] we obtain $a = 0.73$. This value will be used in all DPM calculations. With the WNM we use the parameters in Ref. [26]: $q = 0.4$ GeV and $a = 1.43$. Note that the product aq is the same in both cases. (It turns out that the ratio of J/ψ over DY is very insensitive to the value of a.)

The comparison of $d\sigma^{DY}/dE_T$ with the 1995 data [26] is shown in Fig. 3. The agreement is satisfactory but the error bars are quite large. Also shown is the distribution obtained using the WNM. This correlation has a stronger increase with increasing E_T – but both are consistent with the data within errors.

The comparison with the 1996 E_T distribution is shown in Fig. 4. Again the (statistical) error bars are quite large. Moreover, there is a significant disagreement both with DPM and WNM at $E_T \sim 135$ GeV which was not present when comparing with the 1995 data. There is also a significant difference in shape between DPM and WNM. Note that the only ingredients in the calculation are the b dependence of the DY, $ABT_{AB}(b)$, which is common to all models, plus the $E_T - b$ or $E_T - E_{ZDC}$ correlation. Thus all models which reproduce the latter correlation should lead to the same DY distribution. Since the DPM (with Eqs. ($9'$) or ($9''$) and (10)) gives an excellent description of the latter, the full curve in Fig. 4 should be regarded as the theoretical DY distribution – which can be used as a reference when considering the J/ψ one. Any significant discrepancy with this distribution, such as the one occurring at large E_T, should be regarded as a possible experimental inconsistency between the measured DY E_T distribution and the $E_T - E_{ZDC}$ correlation.

We turn next to the E_T distribution of the J/ψ. We have computed it using $\sigma_{abs} = 6.7$ mb, $\sigma_{co} = 0.6$ mb. The result of our calculation is compared with the 1995 data [26] of the NA50 Collaboration in Fig. 5. The agreement between theory and experiment is reasonable. However the data seem to decrease slightly faster than the theoretical curve. Note that these data show no break in the J/ψ cross-section at any value of E_T. Fig. 5 shows also the E_T distribution obtained with nuclear absorption alone ($\sigma_{abs} = 7.3$ mb) both for DPM (Eq. (9″)) and for the WNM. We see that the shape of the E_T distribution is very sensitive to the effect of the comovers. Thus, a slightly steeper decrease of the J/ψ cross-section, if confirmed, could possibly be obtained with a small increase in the absorption parameters. (The constraint on these parameters coming from the SU data is now significantly smaller due to an increase by a factor 2.8 of the statistical errors; see Section 6.) Note also that, with nuclear absorption alone, the WNM has a faster increase with E_T than the DPM. Therefore the extra J/ψ suppression required in order to reproduce a given shape of the J/ψ distribution, must be considerably stronger in the WNM than in DPM. This is even more clearly seen in Fig. 6 where we compare the theoretical predictions with the J/ψ E_T distribution from the 1996 data in a linear scale. In this comparison we observe some deviations at $E_T \gtrsim 100$ GeV. This region should be studied with great care in the 1998 high statistics run. In our opinion, this is a most interesting region to look for eventual signs of new physics, i.e. for the onset of a truly anomalous suppression at $E_T \gtrsim 100$ GeV. On the contrary, in the region $E_T < 100$ GeV (where the break in the ratio $R(E_T)$ occurs), there is no strong disagreement between theory and experiment. However, there is no perfect agreement either and, therefore, it is not possible to draw a clear conclusion at present. In particular a sudden drop of the J/ψ cross-section at $E_T \simeq 55$ GeV has been claimed [11]. Even if further data show that this drop is statistically significant, our analysis suggests that it cannot be easily attributed to a sudden increase of J/ψ suppression due to deconfinement. Indeed, in the next four E_T bins the measured J/ψ cross-section is consistent with the predictions of a model which does not have deconfinement.

4 J/ψ over DY ratio

The J/ψ suppression is described by the ratio $R(E_T)$ of J/ψ and DY cross-sections in different E_T bins. The advantage of taking this ratio is that systematic errors common to both systems do not appear in this ratio. The inconvenient, however, is that the results are sensitive to the shape of the DY E_T distribution. In our opinion, it is of utmost importance to have good data on the E_T distribution of the J/ψ – as illustrated by the analysis of the previous Section. The ratio $R(E_T)$ is given by

$$R(E_T) = \frac{\int d^2b \ \sigma_{AB}^{\psi}(b) \ P(E_T, b)}{\int d^2b \ \sigma_{AB}^{DY} \ P(E_T, b)} \quad . \tag{14}$$

This ratio has been calculated, within the present model, in Ref. [9], where the values of the parameters (the same ones used here, including the absolute normalization but excepting the value of a which, as discussed in the previous Section, has practically no effect on $R(E_T)$) were determined from the best fit to $R(E_T)$ in pA, SU and $PbPb$ collisions. At that time, however, the 1996 data were not available. The comparison of the model results with both the 1995 and 1996 data [11] is shown in Fig. 7.

The model reproduces the qualitative behavior of the ratio R. However, there are disagreements at a quantitative level. The overall suppression, both from the 1995 and the 1996 data, is somewhat larger than the theoretical one. More important, the 1996 data seem to show a break at $E_T \sim 55$ GeV which is not present in the model calculation. Here, several comments are in order. First, as seen in Fig. 7, the experimental data for the first E_T bin is higher than the one obtained with nuclear absorption alone (with a normalization extracted from a fit to pA and SU data [1, 9]). This is difficult to explain in any model. Second, the relevance of the break at $E_T \sim 55$ GeV is weakened by the existence of fluctuations in $R(E_T)$ at large E_T of a comparable size. These fluctuations, which are generally regarded as spurious, are an example of systematic errors that do not cancel when taking the ratio of J/ψ and DY cross-sections and have to be understood. Third, the failure of the model to describe quantitatively the ratio $R(E_T)$ in the region $E_T \lesssim 100$ GeV is in sharp contrast with the conclusions reached in Section 3 from a direct comparison of the model results with the E_T distribution of the J/ψ which showed reasonable agreement in this E_T region. In order to understand the origin of this contradiction we have plotted in Fig. 8 the theoretical curve of Fig. 7 (full curve), and compared it with the J/ψ suppression obtained from the ratio $\overline{R}(E_T)$ of the experimental E_T distribution of the J/ψ (for the 1996 NA50 data) over the theoretical one for the DY (full curve of Fig. 5). We see that the agreement in shape between theory and experiment has considerably improved; the remaining drop, strongly reduced compared with that of $R(E_T)$, can be attributed to a local minimum in the J/ψ cross-section at $E_T \sim 55$ GeV (difficult to explain in any model, see comments at the end of the previous Section). The ratio $\overline{R}(E_T)$ is now rather well described in the region $E_T < 100$ GeV – except for the first E_T bin. Moreover, in the ratio $\overline{R}(E_T)$ the break at $E_T \sim 55$ GeV has practically disappeared. Fig. 8 indicates that the ratio $R(E_T)$ is very sensitive to the shape of the DY distribution. We would like to stress that Fig. 8 contains no new information. However, it is useful since its comparison with Fig. 7 shows the effect on the ratio $R(E_T)$ of smoothing out the DY cross-section.

Before concluding this section we would like to comment on the modifications in the ratio $R(E_T)$ when using the comover density computed in the WNM, rather than the one based on DPM, Eq. (9). As discussed in Section 2, the WNM underestimates the number of negative particles in a central $PbPb$ collision at $y^* \sim 0$ by $15 \div 30$ %. The corresponding DPM value is 30 % larger than the WNM one and in better agreement with the NA49 data (see Section 2). If we would decrease the density of comovers by 30 % for the most central E_T bin, the value of $R(E_T)$ would decrease by about 10 %. Actually, the net effect would be significantly smaller, since the WNM multiplicity is smaller than the DPM one also in SU, and this can be compensated by a corresponding increase of σ_{co}. Although a difference would remain, it would not basically change the conclusions of the present analysis. On the contrary, our results would be changed if we were to use the WNM in the calorimeter rapidity region, in order to determine the $E_T - E_{ZDC}$ correlation. In this case we would obtain an E_T distribution for the J/ψ which would be too large in the upper half of the E_T interval.

5 Transverse momentum broadening

A mechanism producing an increase of the $\langle p_T \rangle$ of any type of particle produced in pA or AB collisions with increasing nuclear sizes or centrality has been known for a long time [27, 28]. It is due to initial state rescattering. More precisely, for J/ψ production this increase is due to rescattering of the projectile and target gluons, before fusion, with target and projectile nucleons respectively, encountered in their path through the nuclei. The average broadening of the intrinsic gluon distribution in each collision is denoted by δ_0. In Ref. [28] it has been shown that the p_T broadening of the J/ψ is affected by J/ψ absorption. In particular the suppression in $PbPb$ collisions in a deconfining approach [5], produces a maximum in the E_T dependence of $\langle p_T^2 \rangle_{J/\psi}$ at $E_T \sim 100$ GeV followed by a decrease with increasing E_T. This peculiar behavior has been considered as a signature of Quark-Gluon Plasma formation.

In this section, we follow the formalism of p_T broadening of the J/ψ in Ref. [28], but using absorption by comovers instead of the one due to deconfinement.

The broadening of p_T is given by

$$\delta_{AB}(b) \equiv \langle p_T^2 \rangle_{AB}(b) - \langle p_T^2 \rangle_{pp} = N_{AB}(b)\ \delta_0 \quad . \tag{15}$$

N_{AB} is the average number of collisions of the projectile and target gluons with target and projectile nucleons respectively, up to the formation point of the $c\bar{c}$ pair, at fixed b. This point is specified by the impact parameter b and the positions (s, z) and $(b - s, z')$ in the two nuclei. One has

$$N_{AB}(b, s, z, z') = \sigma_{gN} A \int_{-\infty}^{z} dz_A\ \rho_A(s, z_A) + \sigma_{gN} B \int_{-\infty}^{z'} dz_B\ \rho_B(b - s, z_B) \quad . \tag{16}$$

Here σ_{gN} is the gluon-nucleon cross section. This expression (16) has to be averaged over all positions of the $c\bar{c}$ formation point with a weight given by the product of nuclear densities and survival probabilities:

$$W(b, s, z, z') = \rho_A(s, z)\ \rho_B(b - s, z') S_A(s, z)\ S_B(b - s, z')\ S^{co}(b, s) \quad , \tag{17}$$

where

$$S_A(b, z) = \exp\left(-A\sigma_{abs} \int_z^{\infty} d\tilde{z}\ \rho_A(b, \tilde{z})\right) \tag{18}$$

is the survival probability due to nuclear absorption [15] and $S^{co}(b, s)$ is the survival probability due to interaction with comovers, Eq. (2). The latter does not depend on the $c\bar{c}$ formation point.

We obtain in this way

$$N_{AB}(b) = \frac{\int d^2s \int_{-\infty}^{+\infty} dz \int_{-\infty}^{+\infty} dz'\ W(b,s,z,z')\ N_{AB}(b,s,z,z')}{\int d^2s \int_{-\infty}^{+\infty} dz \int_{-\infty}^{+\infty} dz'\ W(b,s,z,z')} \quad . \tag{19}$$

This expression can be written after some transformations as

$$N_{AB}(b) = \sigma_{gN}\ \frac{\int d^2s\ S^{co}(b,s)\,[N_A(s)D_B(b-s) + N_B(b-s)D_A(s)]}{\int d^2s\ S^{co}(b,s)\ D_A(s)\ D_B(b-s)} \quad , \tag{20}$$

where

$$D_A(s) = \frac{1}{A\sigma_{abs}}\,(1 - \exp\,[-A\sigma_{abs}\ T_A(s)]) \tag{21}$$

and

$$N_A(s) = \frac{1}{A\sigma^2_{abs}}\,(\sigma_{abs}AT_A(s) - 1 + \exp\,[-A\sigma_{abs}T_A(s)]) \quad , \tag{22}$$

$D_B = D_A(A \to B)$ and $N_B = N_A(A \to B)$.

Finally, the corresponding quantity at fixed transverse energy can be obtained as

$$N_{AB}(E_T) = \frac{\int d^2b\ P(E_T,b)\ \sigma_{AB}(b)\ N_{AB}(b)}{\int d^2b\ P(E_T,b)\ \sigma_{AB}(b)} \quad , \tag{23}$$

where $P(E_T,b)$ is the $E_T - b$ correlation function, Eq. (11), and $\sigma_{AB}(b)$ is given by Eq. (5).

The values of $\langle p_T^2 \rangle_{pp}$ and $\sigma_{gN}\delta_0$ at 158 AGeV/c are obtained from a fit to the NA50 data [11]. One obtains $\langle p_T^2 \rangle_{pp} = 1.03 \div 1.10$ (GeV/c)^2 and $\sigma_{gN}\delta_0 = 0.39 \div 0.47 \simeq 10.0 \div 12.1$ (GeV fm)^2 (depending on whether the effect of comovers is included or not). The value of $\sigma_{gN}\delta_0 = 0.39$ we obtain for nuclear absorption with $\sigma_{abs} = 7.3$ mb and no comovers, agrees with that obtained in [28], 9.4 ± 0.7 (GeV fm)^2, from a fit to pA and SU data [29, 30]. As suggested in [31], we should take different values of $\langle p_T^2 \rangle_{pp}$ in SU and $PbPb$, since this value increases with energy. Using the values measured [32] in $\pi^- p$ collisions at 150 and 200 GeV/c, the value $\langle p_T^2 \rangle_{pp} = 1.07$ (GeV/c)^2 would correspond to $\langle p_T^2 \rangle_{pp} = 1.23$ (GeV/c)^2 at 200 GeV/c. This last value coincides with the one measured in Ref. [32], 1.23 ± 0.05 (GeV/c)^2, in pp collisions at 200 GeV/c. (From a fit to DY data in pA, OCu, OU and SU [29], a value of $\sigma_{gN}\delta_0 = 0.13$ is obtained, whose ratio over the values for J/ψ is ~ 0.33, smaller than the value $4/9 \simeq 0.44$ suggested [27] by the difference of coupling between gluons and quarks or gluons.)

Our results for nuclear absorption plus comovers with $\sigma_{abs} = 6.7$ mb and $\sigma_{co} = 0.6$ mb (nuclear absorption alone with $\sigma_{abs} = 7.3$ mb), for SU with $\langle p_T^2 \rangle_{pp} = 1.23$ (GeV/c)^2

and $\sigma_{gN}\delta_0 = 0.42$ (0.40), and for $PbPb$ collisions with $\langle p_T^2 \rangle_{pp} = 1.10$ (GeV/c)^2 (in agreement with the mentioned rescaling between 200 and 158 AGeV/c) and the same $\sigma_{gN}\delta_0$ as in SU, are shown in Fig. 9 and compared with experimental data [11, 33]. We see that, in $PbPb$ collisions with comovers, there is a small maximum at $E_T \sim 125$ GeV. However, after this maximum, $\langle p_T^2 \rangle_{AB}$ is practically constant and only slightly smaller than the one obtained with nuclear absorption alone. This is in contrast with the sharper decrease at large E_T found in a deconfining scenario [28]. The physical origin of this decrease is the same in both approaches. At large E_T, corresponding to large comover or energy density, the J/ψ, with large $\langle p_T^2 \rangle$ due to a large number of initial gN collisions, is suppressed by either the comover or the deconfining mechanisms. However, this effect turns out to be numerically much lower in the former approach. Unfortunately, with the present data it is not possible to clearly discriminate between these two predictions.

6 Conclusions and prospects

We have presented a direct comparison of the available NA50 data for the E_T distribution of the J/ψ with the results obtained in a conventional framework based on nuclear absorption plus comover interaction.

Our analysis suggests that the presence of new physics in the region $E_T < 100$ GeV is unlikely. On the contrary, the region $E_T > 100$ GeV is very interesting and should be studied with great care in the 1998 high statistics run. Agreement of the J/ψ cross-section with the comovers results for $E_T \lesssim 100$ GeV together with a significantly sharper decrease for $E_T > 100$ GeV (for which there might be some hint in the 1996 data), would signal the onset of a truly anomalous J/ψ suppression.

Is it possible with the present data to distinguish a deconfining phase transition scenario from the more conventional one described here? In order to answer this question we have to distinguish between deconfining scenarios producing sharp breaks in the ratio $R(E_T)$ [12, 6] from others leading to a smooth behavior of this ratio [3, 4, 5, 6]. For the former, a clear-cut answer will probably come from the 1998 data. On the contrary, it will be more difficult to distinguish the second type of deconfining models from the comover approach presented here.

A very clear way to do so would be to show that the onset of the anomalous suppression is abrupt, i.e. it is not present below some critical density – for instance the maximal one reached in SU collisions [3]. Up to a recent date, there was some evidence for that [11]. Indeed, the effect of the comovers in SU produced a somewhat larger suppression [8, 9] than the measured one. At present, however, the experimental errors in the ratio $R(E_T)$ in SU collisions have been increased by a factor 2.8 (see Ref. [34]; also the experimental errors for $PbPb$ have increased, by a factor 1.4, which has been taken into account in this work). In view of that, it is no longer possible to claim that the J/ψ suppression in SU is too large in the comover approach [9] or that the onset of the anomalous suppression is an abrupt one.

As we have shown in Section 5, there is a difference between comovers and deconfining scenarios regarding the behavior of $\langle p_T^2 \rangle$ versus E_T. According to Ref. [28], in a deconfining scenario this quantity has a maximum at $E_T \sim 100$ GeV and decreases at larger E_T values. In the comover approach presented here, this drop is practically absent and the E_T dependence is close to the one obtained with nuclear absorption alone. Although no such drop is seen in the data, the present experimental errors are rather large and a clear conclusion is not possible.

A promising possibility is the measurement of the J/ψ suppression at higher energies. The J/ψ suppression due to either comover interactions or deconfinement, is expected to increase substantially with increasing energy. In the first case, this is due to the increase of the density of comovers with increasing energy. In the second case, it is due to the corresponding increase of energy density – while the critical value of this quantity is unchanged. Therefore, it is important to make predictions at higher energies in both approaches, using the values of the parameters determined from present data. One can hope that the differences in the predictions of the two approaches will be sufficiently large to be experimentally measurable.

The main uncertainty in the determination of the absolute value of the suppression at high energies resides in the value of dN/dy at $y^* \sim 0$. For instance, in central $PbPb$ collisions, at RHIC energies, one expects in DPM a value [35] for negative particles $dN^-/dy|_{y^*\sim 0} = 1000$, and 3500 at $\sqrt{s_{NN}} = 5.5$ TeV. On the contrary, from the scaling in the number of participants (WNM) one expects a value $dN^-/dy|_{y^*\sim 0} = 400$ at $\sqrt{s_{NN}} = 200$ GeV and 800 at $\sqrt{s_{NN}} = 5.5$ TeV. In the first case, there is an increase by roughly a factor 5 at RHIC (17.5 at LHC) with respect to the value at $\sqrt{s_{NN}} = 17$

GeV. In the second case, there is only an increase by a factor 2 at RHIC (4 at LHC), which is due to the corresponding increase of $dN/dy|_{y^*\sim 0}$ in pp collisions. An estimate at RHIC (LHC) of the J/ψ survival probability in central $PbPb$ collisions is given in Table 1. The numbers in this Table, for comover absorption alone, are obtained from Eq. (2) by rising the comover absorption, computed at $\sqrt{s_{NN}} = 17$ GeV for a central E_T bin ($E_T \sim 145$ GeV), to a power 2 (4) in the case of the WNM and to a power 5 (17.5) in the case of DPM. The corresponding numbers for the total J/ψ suppression are obtained by multiplying the ones for comovers alone given in Table 1, by the nuclear absorption. The latter is expected to depend little on energy [36].

These estimates illustrate the important increase of the J/ψ suppression with energy and also the dramatic uncertainties associated to the value of $dN/dy|_{y^*\sim 0}$. Clearly, a more detailed calculation is needed which takes into account the modifications of parton densities inside nuclei (usually neglected at SPS energies) and also the changes in the Glauber formulae due to the increase with energy of σ_{pp}. However, it is obvious that the J/ψ suppression will increase strongly with increasing energies and it is very unlikely that the results will be the same in the comover and in the deconfining frameworks.

Acknowledgments: It is a pleasure to thank A. B. Kaidalov, A. Krzywicki, C. A. Salgado, Yu. M. Shabelski and J. Trân Thanh Vân for discussions, and F. Bellaiche, B. Chaurand, C. Gerschel, M. Gonin, C. Lourenço and A. Romana for discussions and useful information on the experimental data. N. A. thanks Dirección General de Investigación Científica y Técnica of Spain for financial support and J. Hernández, M. Martínez, J. Puga, J. Roldán and J. Terrón for discussions on experimental aspects. E. G. F. thanks Fundación Ramón Areces of Spain for financial support. A. C. acknowledges partial support from NATO grant OUTR.LG971390 and INTAS grant 93-79. Laboratoire de Physique Théorique et Hautes Energies is Laboratoire associé au Centre National de la Recherche Scientifique – URA D00063.

References

[1] NA50 Collaboration: M. C. Abreu *et al.*, Phys. Lett. **B410**, 327 (1997); 337.

[2] T. Matsui and H. Satz, Phys. Lett. **B178**, 416 (1986).

[3] J.-P. Blaizot and J.-Y. Ollitrault, Phys. Rev. Lett. **77**, 1703 (1996); Nucl. Phys. **A610**, 452c (1996).

[4] C.-Y. Wong, Nucl. Phys. **A610**, 434c (1996); Phys. Rev. **C55**, 2621 (1997).

[5] D. Kharzeev, C. Lourenço, M. Nardi and H. Satz, Z. Phys. **C74**, 307 (1997).

[6] R. Vogt, Phys. Lett. **B430**, 15 (1998). In this article it is claimed that nuclear absorption plus comover interaction cannot explain the size of the J/ψ suppression observed in $PbPb$ collisions. An opposite conclusion is reached in [9] and in the present work. In [6] the Wounded Nucleon Model is used to compute the comovers suppression as well as the $E_T - b$ correlation. Another difference resides in the value of the absorptive cross-section – which is taken to be equal to 4.8 mb in Ref. [6] and 6.7 mb in our case.

[7] S. Gavin and R. Vogt, Nucl. Phys. **A610**, 442c (1996); Phys. Rev. Lett. **78**, 1006 (1997). One of the authors (R.V.) has claimed [6] that this work has an error in the relative normalizations in SU and $PbPb$ collisions which invalidates its conclusions.

[8] A. Capella, A. B. Kaidalov, A. Kouider Akil and C. Gerschel, Phys. Lett. **B393**, 431 (1997).

[9] N. Armesto and A. Capella, Phys. Lett. **B430**, 23 (1998); J. Phys. **G23**, 1969 (1997); N. Armesto, in Proceedings of the XXXIInd Rencontres de Moriond, edited by J. Trân Thanh Vân (Editions Frontières, Paris, 1997), p. 519.

[10] W. Cassing and C. M. Ko, Phys. Lett. **B396**, 39 (1997); W. Cassing and E. L. Bratkovskaya, in Proceedings of the XXXIInd Rencontres de Moriond, *ibid*, p. 531; Nucl. Phys. **A623**, 570 (1997); J. Geiss, C. Greiner, E. L. Bratkovskaya, W. Cassing and U. Mosel, nucl-th/9803008.

[11] NA50 Collaboration: L. Ramello at Quark Matter '97, Tsukuba, Japan, December 1997; M. Gonin at Probes of Dense Matter in Ultrarelativistic Heavy Ion Collisions, Seattle, USA, May 1998.

[12] D. Kharzeev, M. Nardi and H. Satz, preprint BI-TP 97/33 (hep-ph/9707308); M. Nardi and H. Satz, preprint BI-TP 98/10 (hep-ph/9805247).

[13] T. Matsui, presented at Quark Matter '97, *ibid.*

[14] S. Frankel and W. Frati, hep-ph/9710532; R. C. Hwa, J. Pišút and N. Pišútová, Phys. Rev. **C56**, 432 (1997); **C58**, 434 (1998); H. Sorge, E. Shuryak and I. Zahed, Phys. Rev. Lett. **79**, 2775 (1997).

[15] A. Capella, J. A. Casado, C. Pajares, A. V. Ramallo and J. Trân Thanh Vân, Phys. Lett. **B206**, 354 (1988); A. Capella, C. Merino, J. Trân Thanh Vân, C. Pajares and A. V. Ramallo, Phys. Lett. **B243**, 144 (1990).

[16] C. W. de Jager, H. de Vries and C. de Vries, Atomic Data and Nuclear Data Tables **14**, 479 (1974).

[17] P. Koch, U. Heinz and J. Pišút, Phys. Lett. **B243**, 149 (1990).

[18] A. Capella, Phys. Lett. **B364**, 175 (1995); A. Capella, A. B. Kaidalov, A. Kouider Akil, C. Merino and J. Trân Thanh Vân, Z. Phys. **C70**, 507 (1996).

[19] S. J. Brodsky and A. H. Mueller, Phys. Lett. **B206**, 685 (1988).

[20] NA38 Collaboration: C. Baglin *et al.*, Phys. Lett. **B251**, 472 (1990).

[21] A. Bialas, in Proceedings of the XIIIth International Symposium on Multiparticle Dynamics, edited by W. Kittel, W. Metzger and A. Stergiou (World Scientific, Singapore, 1983), p. 328.

[22] For a review see A. Capella, U. P. Sukhatme C.-I. Tan and J. Trân Thanh Vân, Phys. Rep. **236**, 225 (1994).

[23] NA49 Collaboration: presented by G. Roland at Quark Matter '97, *ibid.*

[24] NA35 Collaboration: T. Alber *et al.*, preprint IKF-HENPG/6-94 (July 1997); M. Gaździcki and D. Röhrich, Z. Phys. **C65**, 215 (1995).

[25] A. Bialas, M. Bleszyński and W. Czyz, Nucl. Phys. **B111**, 461 (1976).

[26] F. Bellaiche (NA50 Collaboration), Ph.D. Thesis, Université de Lyon, France, 1997.

[27] A. Krzywicki, J. Engels, B. Petersson and U. P. Sukhatme, Phys. Lett. **85B**, 407 (1979); S. Gavin and M. Gyulassy, Phys. Lett. **B214**, 241 (1988); J.-P. Blaizot and J.-Y. Ollitrault, Phys. Lett. **B217**, 392 (1989); S. Gupta and H. Satz, Phys. Lett. **B283**, 439 (1992); S. Gavin and R. Vogt, preprint CU-TP-791 (hep-ph/9610432); see also Ref. [3].

[28] D. Kharzeev, M. Nardi and H. Satz, Phys. Lett. **B405**, 14 (1997).

[29] NA38 Collaboration: C. Baglin *et al.*, Phys. Lett. **B262**, 362 (1991).

[30] R. Mandry (NA38 Collaboration), Ph.D. Thesis, Université Claude Bernard, Clermont-Ferrand, France, 1993.

[31] C. Gerschel and J. Hüfner, hep-ph/9802245.

[32] NA3 Collaboration: J. Badier *et al.*, Z. Phys. **C20**, 101 (1983).

[33] NA38 Collaboration: M. C. Abreu *et al.*, Phys. Lett. **B423**, 207 (1998).

[34] NA50 Collaboration: presented by A. Romana at the XXXIIIrd Rencontres de Moriond, Les Arcs, France, March 1998.

[35] A. Capella, C. Merino and J. Trân Thanh Vân, Phys. Lett. **B265**, 415 (1991).

[36] M. A. Braun, C. Pajares, C. A. Salgado, N. Armesto and A. Capella, Nucl. Phys. **B509**, 357 (1998).

Table captions:

Table 1. Comover and total J/ψ suppression at SPS, RHIC and LHC, for central $PbPb$ collisions, in the WNM and the DPM (see text for an explanation).

Table 1

	SPS Comover	SPS Total	RHIC Comover	RHIC Total	LHC Comover	LHC Total
WNM	0.62	0.23	0.38	0.14	0.14	0.06
DPM	0.62	0.23	0.09	0.03	$2 \cdot 10^{-4}$	$8 \cdot 10^{-5}$

Figure captions:

Figure 1. Rapidity distribution of negative hadrons in central $PbPb$ collisions at 158 AGeV/c. Preliminary data of the NA49 Collaboration [23] (black circles) are compared with the DPM results (solid line) using the same centrality criterium, and with the scaling in the number of participants (dashed line [23]).

Figure 2. $E_T - E_{ZDC}$ correlation: the full line is obtained in DPM from Eqs. (9′′) and (10) and gives a very good description of the NA50 collaboration data [11]. The dotted line is obtained in DPM from Eqs. (9) and (10). The dashed line is obtained in the WNM with $E_T(b) = 0.4\ [m_A(b) + m_B(b)]$ GeV [5].

Figure 3. Inclusive cross-section $d\sigma^{DY}/dE_T$ for DY pair production with $M_{\mu\mu} > 4.2$ GeV/c^2 from the 1995 NA50 data [26] compared to the results obtained from Eq. (12) with $\sigma_{abs} = \sigma_{co} = 0$. The full curve is obtained in DPM and the dashed one in the WNM. The normalization constant $\sigma_{pp}^{DY}/\sigma_{pp}$ in Eq. (3) is $9 \cdot 10^{-10}$. Note that, in order to compare with the experimental value of $\sigma_{pp}^{DY}/\sigma_{pp}$, this normalization factor should be divided by 5 due to the E_T binning in Fig. 3.

Figure 4. Preliminary E_T distribution dN^{DY}/dE_T for DY pair production with $M_{\mu\mu} >$ 4.2 GeV/c^2 for the 1996 NA50 data [11] compared to the theoretical curves of Fig. 3 normalized to the data. The common normalization factor is 0.10 fm^{-2}.

Figure 5. Inclusive cross-section $d\sigma^{J/\psi}/dE_T$ for J/ψ production from the 1995 NA50 data [26] compared with the results obtained from Eq. (12). The normalization constant $B_{\mu\mu}\sigma_{pp}^{J/\psi}/\sigma_{pp}$ in Eq. (3) is $2.4 \cdot 10^{-7}$. The dotted line is obtained with nuclear absorption alone ($\sigma_{abs} = 7.3$ mb, $\sigma_{co} = 0$), while the solid line contains the effect of comovers with $\sigma_{abs} = 6.7$ mb and $\sigma_{co} = 0.6$ mb. The dashed line is obtained in the WNM with nuclear absorption alone ($\sigma_{abs} = 7.3$ mb, $\sigma_{co} = 0$).

Figure 6. Premiminary E_T distribution $dN^{J/\psi}/dE_T$ for J/ψ production from the 1996 NA50 data [11], compared with the theoretical curves of Fig. 5 normalized to the data.

The common normalization factor is 5.57 fm^{-2}. The circles and the crosses correspond to two different experimental methods [11]: fitting and counting procedures.

Figure 7. The ratio $R(E_T)$ of J/ψ over DY versus E_T both from the 1995 [1] (open symbols) and preliminary 1996 [11] (black symbols) NA50 data compared to the ratio of theoretical curves (solid lines) in Figs. 4 and 6 (with comovers, solid line). The dotted line is obtained in DPM with nuclear absorption alone (σ_{abs} = 7.3 mb, σ_{co} = 0). The normalization factor (61.2) is the one obtained in [9] from a fit to the pA, SU and $PbPb$ data. This normalization coincides with the one obtained from the normalizations of the individual E_T distributions in Figs. 4 and 6 after correcting the latter for the different E_T binnings, the experimental acceptances and the different DY mass range – which is $2.9 < M < 4.5$ GeV/c^2 in the ratio $R(E_T)$ and $M > 4.2$ GeV/c^2 in Fig. 4.

Figure 8. The theoretical curve of Fig. 7 (solid line) is compared to the ratio $\overline{R}(E_T)$ of the experimental E_T distribution of Fig. 6 over the theoretical DY distribution of Fig. 4 (solid line). Here the normalization of $\overline{R}(E_T)$ is arbitrary – since we are only interested in the change in the shape of $R(E_T)$ when smoothing the DY E_T distribution.

Figure 9. $\langle p_T^2 \rangle_{AB}$ in a) SU and b) $PbPb$ collisions at SPS. Solid line: nuclear absorption plus comovers; dotted line: nuclear absorption alone (see text for the values of the corresponding parameters). Black circles are experimental data from [11, 33].

Figure 1

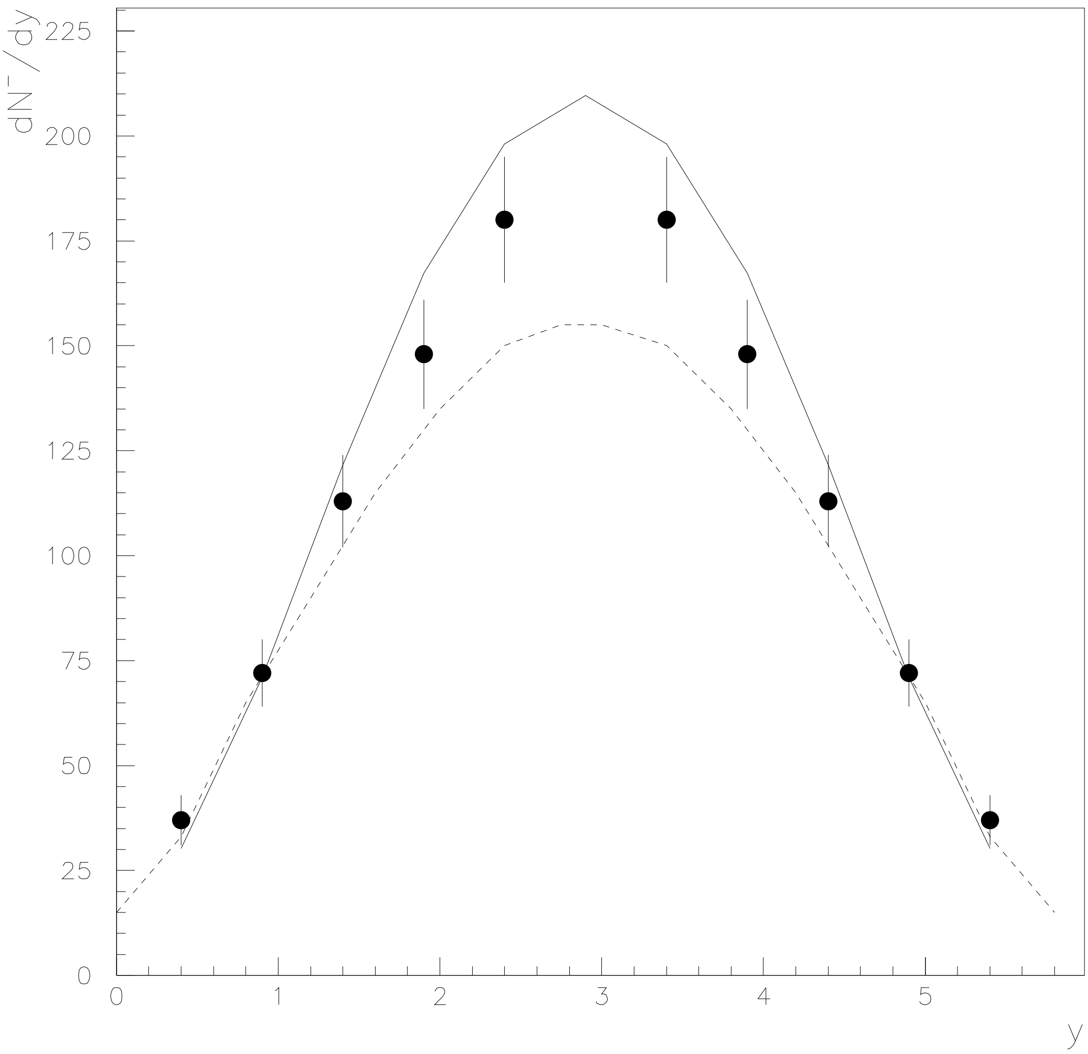

Figure 2

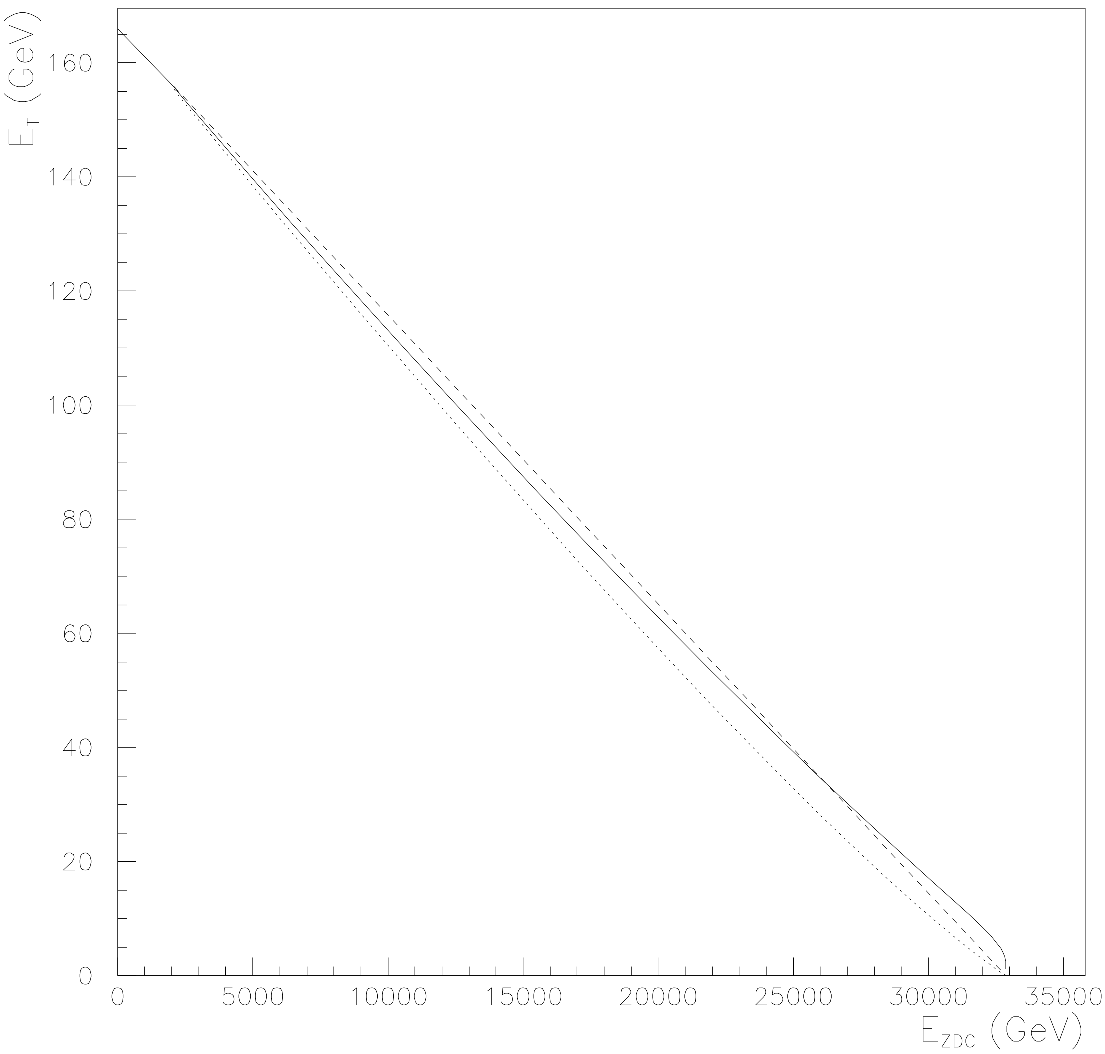
E_T (GeV)
160
140
120
100
80
60
40
20
0
0
5000
10000
15000
20000
25000
30000
35000
E_ZDC (GeV)

Figure 3

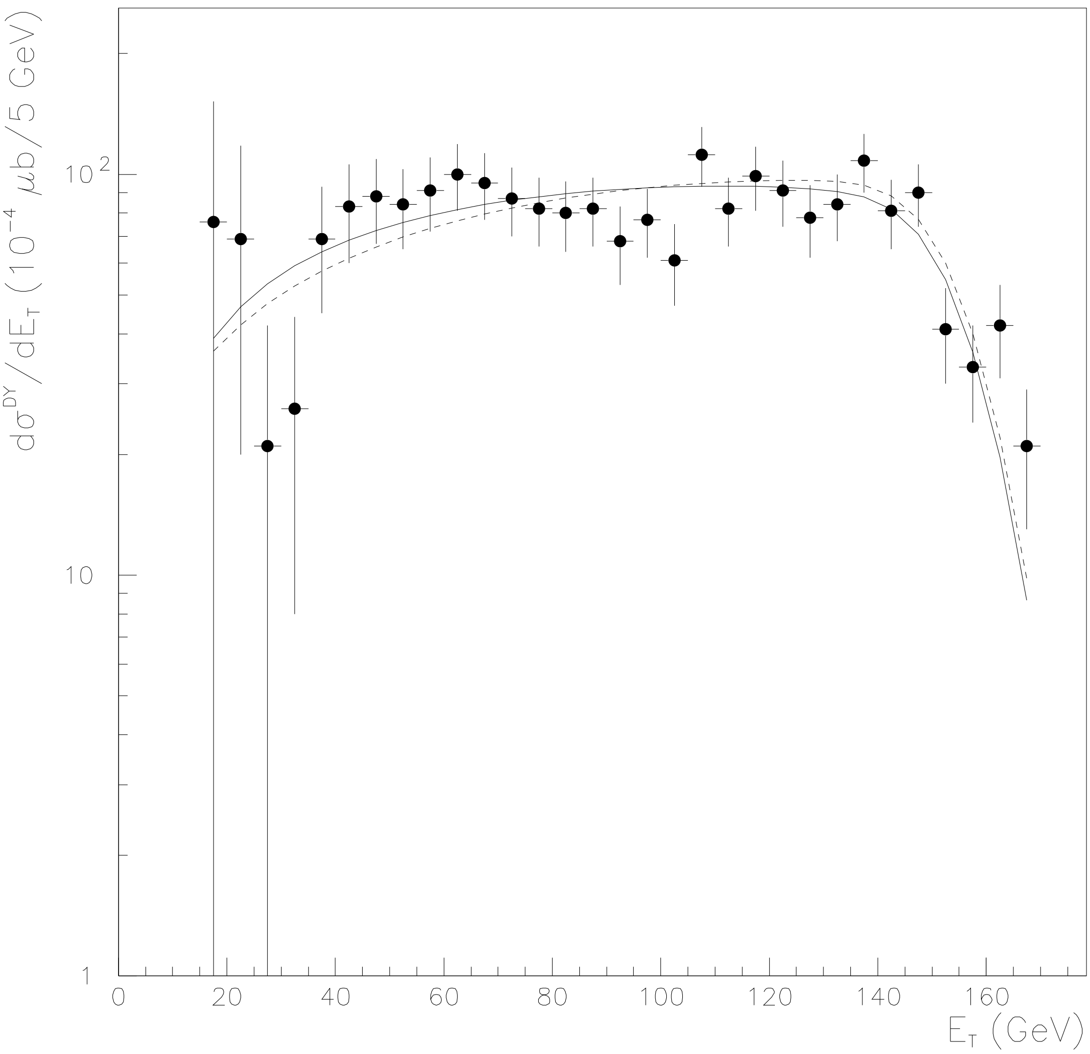

$d\sigma^{DY}/dE_T$ (10^{-4} μb/5 GeV)
10^2
10
1
0
20
40
60
80
100
120
140
160
E_T (GeV)

Figure 4

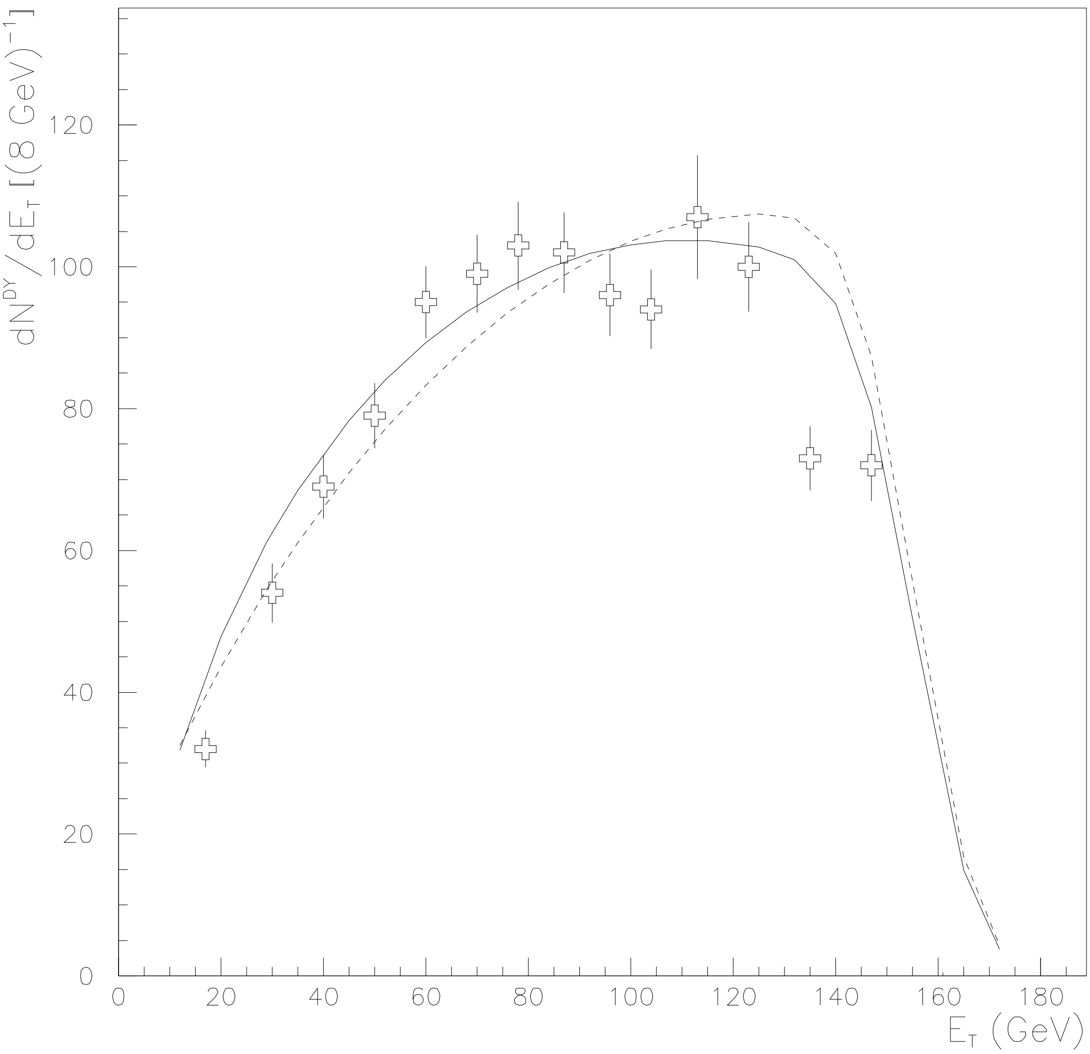

dN^DY/dE_T [(8 GeV)^-1]
0
20
40
60
80
100
120
0
20
40
60
80
100
120
140
160
180
E_T (GeV)

Figure 5

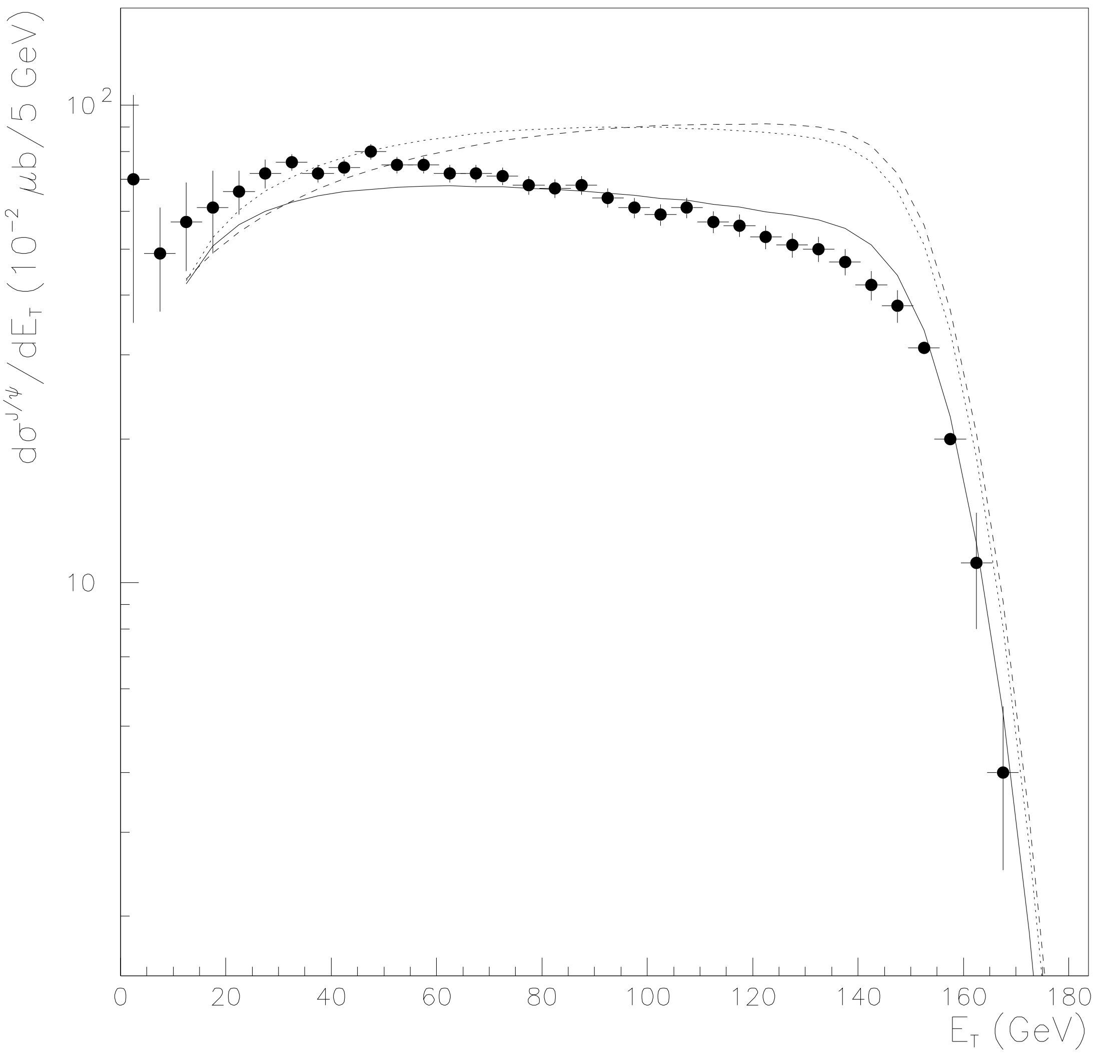

$d\sigma^{J/\psi}/dE_T$ (10^{-2} μb/5 GeV)
10^2
10
0
20
40
60
80
100
120
140
160
180
E_T (GeV)

Figure 6

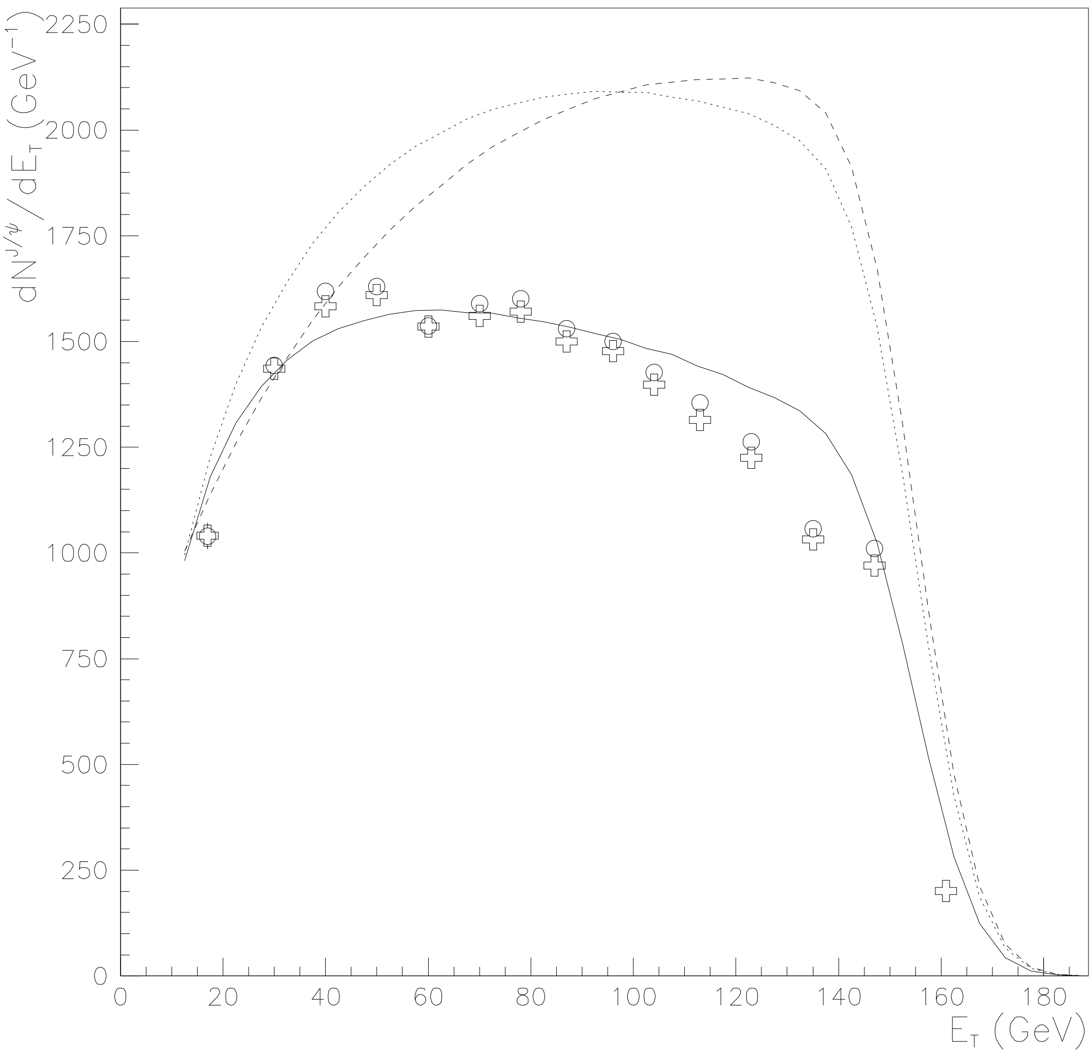

2250
2000
1750
1500
1250
1000
750
500
250
0
0
20
40
60
80
100
120
140
160
180
$dN^{J/\psi}/dE_T\,(GeV^{-1})$
E_T (GeV)

Figure 7

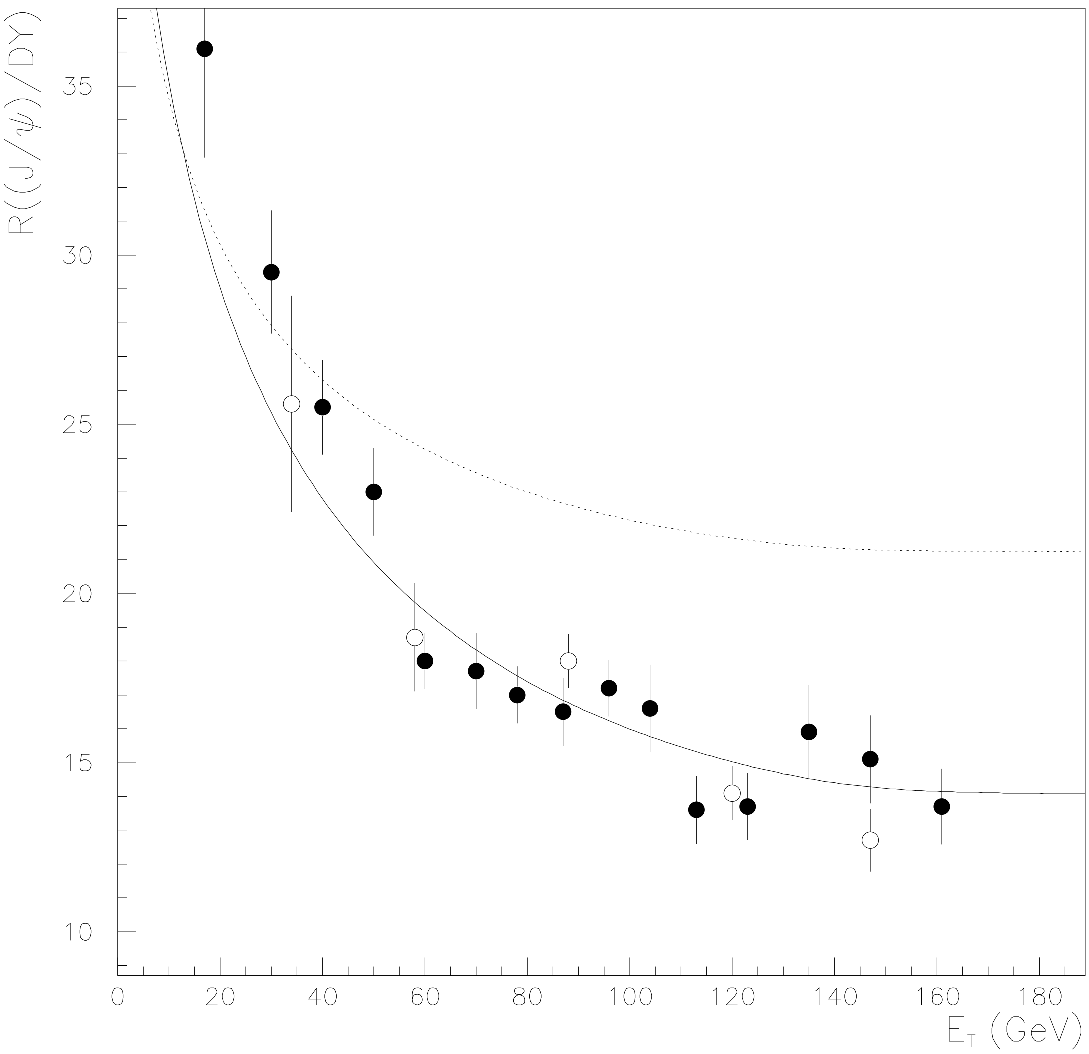

Figure 8

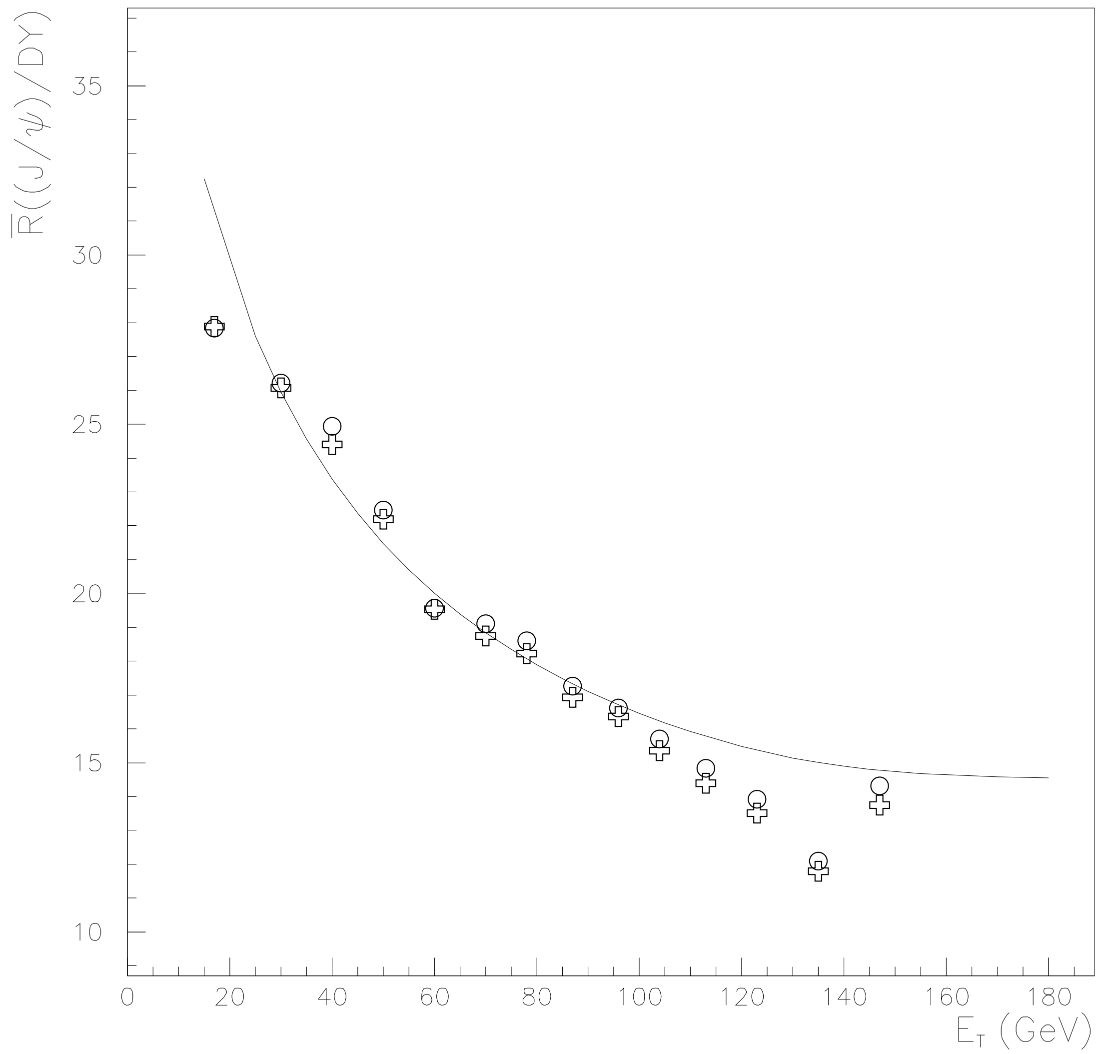

$\overline{R}((J/\psi)/DY)$
35
30
25
20
15
10
0
20
40
60
80
100
120
140
160
180
E_T (GeV)

Figure 9

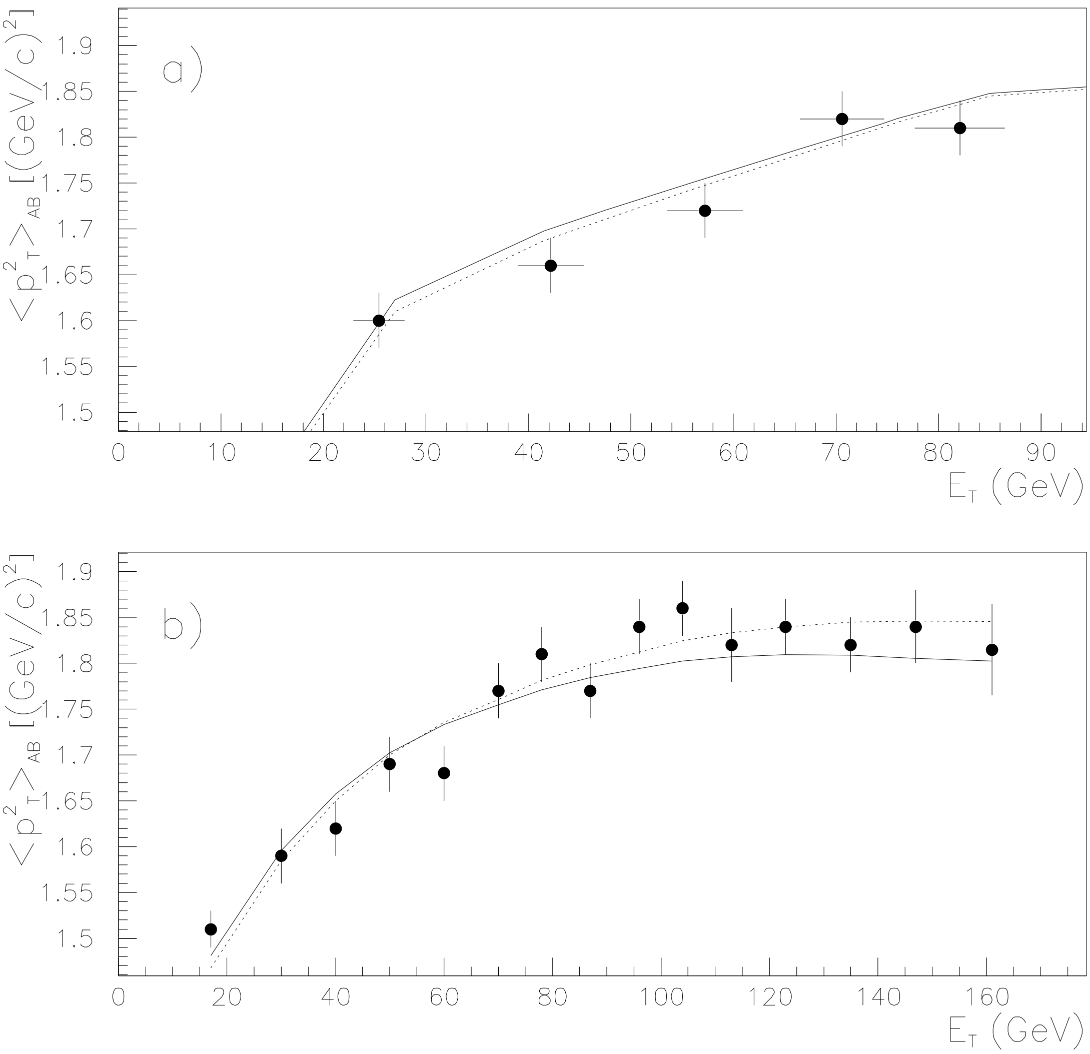
a)
b)
$<p_T^2>_{AB}$ [(GeV/c)^2]
E_T (GeV)
1.5
1.55
1.6
1.65
1.7
1.75
1.8
1.85
1.9
0
10
20
30
40
50
60
70
80
90
100
120
140
160